

## CRATER DEGRADATION AND SURFACE EROSION RATES AT THE INSIGHT LANDING SITE, WESTERN ELYSIUM PLANITIA, MARS.

J. Sweeney<sup>1</sup>, N.H. Warner<sup>1</sup>, M.P. Golombek<sup>2</sup>, R. Kirk<sup>3</sup>, R.L. Fergason<sup>3</sup>, A. Pivarunas<sup>1</sup>, <sup>1</sup>State University of New York at Geneseo, 1 College Circle, Geneseo, NY, <sup>2</sup>Jet Propulsion Laboratory, California Institute of Technology, Pasadena, CA, <sup>3</sup>U.S. Geological Survey, Flagstaff, AZ. warner@geneseo.edu & jms60@geneseo.edu.

**Introduction:** Methods used for estimating erosion rates on Mars include in situ rover-based observations of crater modification as well as orbital analyses of crater morphology and related landforms [1- 4]. For small craters, the latter method has been limited by the resolution of available imagery and lack of high resolution topography data. Global and regional degradation rates have been inferred from orbital data using km-size impact craters over broad regions of the surface. For rover-based observations, most estimates of degradation have been made locally, and for craters smaller than 100 m in diameter.

Here, we analyze the preservation and degradation timescales of (order of) 100-m-scale impact craters using high-resolution imagery and topographic data from the High Resolution Imaging Science Experiment (HiRISE) made available by the InSight landing site selection process. The final landing region for InSight is in southwestern Elysium Planitia on Early Hesperian-age, ridged volcanic plains. The terrains here exhibit no evidence for fluvial, lacustrine, glacial, or periglacial activity, suggesting that surface processes are limited to impact gardening and aeolian modification [5]. Our study therefore is an evaluation of how 100-m-scale craters degrade over time on Mars in an environment that is most typical of an equatorial, Hesperian to Amazonian-age climate.

**Methods:** Three HiRISE images (25 cm pixel<sup>-1</sup>) covering an area of 3.45 x 10<sup>4</sup> km<sup>2</sup> were analyzed within the final InSight landing ellipse (Fig. 1).

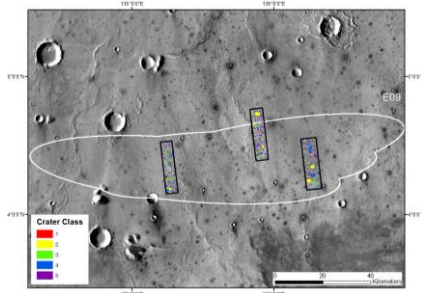


Figure 1: THEMIS Daytime IR image (100 m pixel<sup>-1</sup>) showing the location of the three HiRISE images within the final 2016 InSight landing ellipse.

Here, we examine the degradation states of all craters above ~100 m in size within these images. Craters of this size in this region are noted for their rocky ejecta blankets, indicating the presence of a competent bedrock layer at depth [6].

In total, 595 craters were mapped from the images and their relative degradation states classified based on observed geomorphic characteristics of their ejecta blankets and crater rims (Fig. 2) [6]. Class 1 craters for example represent an idealized, pristine, simple crater. These craters have an elevated crater rim that is 100% continuous around its circumference, no floor infill (aeolian materials or dust), limited evidence for interior mass wasting, and rocks in their ejecta blanket that extend roughly one diameter from the rim. Very few Class 1 craters were mapped over the region. Class 2 craters represent the freshest examples and are common in the region. Class 2 craters also exhibit a near continuous crater rim and ejecta blanket but show some evidence for both exterior and interior modification.

Along the spectrum of degradation, the more degraded classes display more discontinuous crater rims, a higher abundance of superimposed meter to ten-meter scale craters, a transition from infilling bedforms to near complete infilling by smooth material, and a reduction in the abundance and continuity of rocks in the ejecta blanket. The most degraded class analyzed here is our Class 5 crater which still exhibits rocks in its ejecta blanket. We did not evaluate more-degraded Class 6 craters that lack rocks in their ejecta blanket.

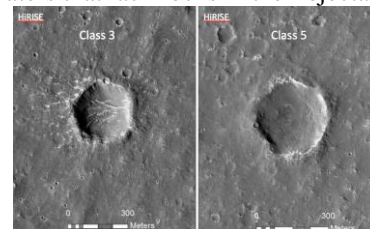


Figure 2: HiRISE images showing a 300 m Class 3 crater and a 300 m Class 5 crater.

To quantify and test our visual classification we utilized three 1 m HiRISE DEMs constructed for the InSight landing site assessment [7]. These were co-registered with our three HiRISE images. From the DEMs, we measured crater diameter (D), depth (d) and rim height (R). Mean values for D and d were measured for each of the 595 craters from four topographic profiles constructed in N-S, E-W, NE-SW, and NW-SE directions. Rim height (R) was measured for a subset of 207 craters, including all Class 2 and Class 3 craters. A mean rim height was measured at eight points around the crater rim from the rim peak to a distance approximately one crater diameter from the rim.

To estimate the timescales of degradation, we plotted the size-frequency distribution (SFD) of all crater classes. Using standard production and chronology functions for Mars [8,9], we determined the time required to degrade a crater from a pristine Class 2 state to the state of a Class 5 crater. From the crater morphology measurements and timescales, we calculated crater degradation and rim erosion rates for this region.

**Results:** Figure 3 shows the depth ( $d$ ) and diameter ( $D$ ) measurements from the HiRISE DEMs plotted on log-log axes. The data for the most pristine Class 2 craters exhibits a power law trend that gives the expression:  $d = 0.0613D^{1.0822}$  ( $R^2 = 0.9457$ ). The color code here illustrates our visual classification of crater morphology. The plot demonstrates that our visual classification from HiRISE closely matches the  $d/D$  data measured from the DEMs. In other words, the DEMs confirm our confidence in the observational classification of crater morphology.

By comparing the depths of Class 2 and Class 5 craters we determined the average amount of crater degradation that occurs between these two end members. For example, for a crater with  $D = 200$  m, we measured an average of 14 m of degradation between Class 2 and Class 5 craters. From the SFD plot (Fig. 4), we found that modification from a fresh Class 2 crater to a degraded Class 5 crater of a similar diameter requires  $600 \pm 90$  Ma (Fig. 4). Using the total amount of degradation with this timescale we calculated a crater degradation rate of 0.02 m/Myr for the InSight landing site.

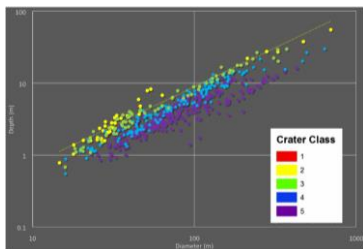


Figure 3: Measurements of REC depth and diameter ( $n = 595$ ).

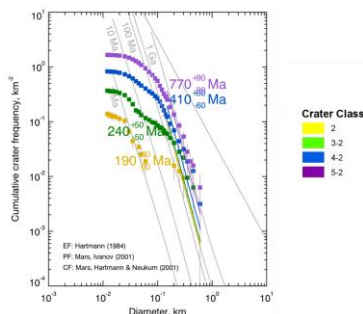


Figure 4: SFD plot for all RECs in the three HiRISE images.

By comparison, rim height measurements suggest that a 200 m sized crater in this region experienced on

average only 5 m of degradation between a Class 2 and Class 5 state. Over the same timescales of 600 Myr, this provides a rim degradation rate of only 0.008 m/Myr. From a similar R/D plot we calculated a power law relationship of:  $R = 0.0098D^{1.1867}$  ( $R^2 = 0.8019$ ).

**Discussion and Conclusions:** The crater degradation rate of 0.02 m/Myr accounts for both rim degradation as well as infill of the crater floor. By comparison, the rim degradation rate, which is likely dominantly the result of rim erosion by aeolian process, is an order of magnitude lower at 0.008 m/Myr. Both the degradation and rim erosion rates are low and are similar to rates calculated for other Hesperian to Amazonian aged-terrains [1, 2]. However, the data indicate that rim erosion at the InSight landing site is outpaced by crater infilling processes. In many cases, Class 5 craters are infilled to the elevation of the surrounding terrain while still maintaining both rocks in their ejecta blankets and remnants of an elevated rim. Our observations suggest that erosion rates that are estimated using only crater depth to diameter relationships may over-estimate the influence of erosive processes on the surface of Mars.

Erosion rates were also calculated between each crater class interval to determine how the pace of degradation changes as craters age. For both the crater degradation rate and rim erosion rate, there is a decrease in the rate of degradation over time. For example, as a crater is modified from a Class 2 state to a Class 3 state, the degradation rate is 0.07 m/Myr and the rim erosion rate is 0.04 m/Myr. However, as a crater is modified from a Class 4 state to a Class 5 state, the degradation and rim erosion rates are much slower: 0.02 m/Myr and 0.002 m/Myr, respectively. The decrease in degradation rates over time is likely caused by the degradation process itself. As craters degrade and their rims erode they become less of a topographic obstacle to aeolian processes. Crater rims are reduced in size and height and the crater floor fills until it is flat with the surrounding terrain. More ancient, shallow craters therefore trap less sediment and the rims themselves provide less material to erode. Estimates of crater degradation and erosion rates elsewhere on Mars should therefore consider these time-dependent relationships.

**References:** [1] Golombek, M.P. et al. (2014) *JGR* 119. [2] Golombek, M.P. et al. (2006) *JGR* 111. [3] Warner, N.H. et al. (2010) *JGR* 115. [4] Carr, M.H. (1992) *23<sup>rd</sup> LPSC*, 205-206. [5] Wigton, N.R. et al. (2014) *45<sup>th</sup> LPSC*, #1234. [6] Warner et al. (2016) *47<sup>th</sup> LPSC*, this conference. [7] Howington-Kraus, E., et al. (2015) *46<sup>th</sup> LPSC*, Abstract #2435. [8] Ivanov, B. (2001) *Space Sci. Rev.* 96, 87-104. [9] Hartmann, W.K. and Neukum, G. (2001) *Space Sci. Rev.* 96, 165-194.